Available online at www.sciencedirect.com
SCIENCE DIRECT®
International Journal of Heat and Fluid Flow 25 (2004) 444–450
International Journal of HEAT AND FLUID FLOW
www.elsevier.com/locate/ijhff

Parameters controlling roughness effects in a separating boundary layer

Carolyn D. Aubertine [a,*], John K. Eaton [a], Simon Song [b]

[a] Department of Mechanical Engineering, Stanford University, Stanford, CA 94305-3030, USA
[b] Sandia National Laboratory, Livermore, CA 94551-9951, USA

Abstract

The effects of wall roughness were examined experimentally for two different rough-wall cases involving flow over a ramp with separation and reattachment. For these cases, the roughness Reynolds number was matched at two different momentum thickness Reynolds numbers. Both flow conditions were fully rough. The effect of increasing the wall roughness was to increase the friction velocity and increase the separation region size. The two rough-wall cases produced different size separation regions and different friction velocity values. This shows that the roughness Reynolds number is not sufficient to characterise the roughness effects. Another parameter such as the ratio of the roughness height to the boundary layer thickness is also necessary. In both cases, the outer layer turbulence was mainly affected by the change in the friction velocity.

Keywords: Turbulent boundary layer; Separation; Roughness effects; Reynolds number effects

1. Introduction

While many laboratory experiments are performed over smooth surfaces, practical surfaces are often rough. This is especially true for large-scale vehicles that operate at very high Reynolds numbers. As the viscous length scale decreases with increasing Reynolds number, the roughness height becomes more important. At high Reynolds numbers, all but extremely smooth surfaces are hydrodynamically rough. The effect of the roughness is to increase the skin friction, and thus the boundary layer momentum deficit. This may affect separation behavior, and thereby overall vehicle performance.

The effects of roughness have been studied extensively for pipe flows and flat plate boundary layers. A recent review of roughness research performed in zero pressure gradient boundary layers by Raupauch et al. (1991) examined both atmospheric and laboratory flows. The type of roughness varied and included meshes, screens and perforated plates (Krogstad and Antonia, 1999; Perry et al., 1987; Tachie et al., 2000), uniform spheres (Ligrani and Moffat, 1986), grooves of a variety of dimensions (Bandyopadhyay, 1987; Keirsbulck et al., 2002; Perry et al., 1969) wavy machined surfaces (Perry et al., 1987), uniform sandgrains (Bandyopadhyay, 1987; Bergstrom et al., 2002; Tachie et al., 2000) and sandpaper (Song and Eaton, 2002a). In general, for each new roughness geometry, it is necessary to determine the effective roughness height and the virtual origin of the boundary layer. Thus far, no theory is available to predict these quantities given only a geometric specification of the roughness.

Roughness is often characterised based on how it affects the flat plate mean velocity profile, which may be matched to a modified log law as:

$$\frac{U}{U_\tau} = \frac{1}{\kappa}\ln\left(\frac{yU_\tau}{\nu}\right) + B - \Delta\frac{U}{U_\tau} \tag{1}$$

where κ and B are standard log law constants and y is measured from a virtual origin located somewhere above the base level of the roughness (Ligrani and Moffat, 1986; Perry et al., 1969). The last term is called the roughness function, and shifts the velocity profile down in a standard law of the wall plot. Matching the velocity profile to this form is difficult because both the friction velocity and the y-origin shift are unknown.

* Corresponding author. Tel.: +1-650-723-8556; fax: +1-650-723-4548.
E-mail addresses: caubertine@stanford.edu (C.D. Aubertine), eaton@vonkarman.stanford.edu (J.K. Eaton), ssong@sandia.gov (S. Song).

0142-727X/$ - see front matter © 2004 Elsevier Inc. All rights reserved.
doi:10.1016/j.ijheatfluidflow.2004.02.007

Various methods of fitting the velocity profile (Krogstad and Antonia, 1999; Perry et al., 1987; Tachie et al., 2000), a momentum integral analysis (Ligrani and Moffat, 1986) and extrapolation of the total shear stress (Song and Eaton, 2002a) have all been used to determine the friction velocity. None of these techniques is entirely satisfactory, and in the absence of direct shear force measurements, the uncertainty in U_τ is fairly large. In recent work, Smalley et al. (2002) have questioned the utility of characterising roughness effects based solely on mean velocity measurements.

Boundary layers are divided into smooth, transitionally rough and fully rough regimes, based on the roughness Reynolds number, which is the ratio of the roughness height to the viscous length scale. For smooth boundary layers, the roughness Reynolds number is less than 5–10 and for fully rough boundary layers the roughness Reynolds number is greater than 55–90. Ligrani and Moffat (1986) used an equivalent sandgrain roughness k_s, rather than k, for these limits. This equivalent sandgrain height relates the actual roughness height to the uniform sandgrain size used in Nikuradse's experiments for pipe flows, giving the same value of the roughness function ($\Delta U/U_\tau$). Some of the previous work implies then that roughness effects are fully determined by the roughness Reynolds number, although there is no work showing that roughness effects are independent of other length scales such as the roughness height divided by the boundary layer thickness.

Another open question is the effect that roughness has on both the mean velocity and turbulent stresses far away from the wall. The idea of wall similarity was proposed by Townsend (1976) and further discussed by Raupauch et al. (1991) who observed that far from the wall, the roughness has no effect on the flow other than to change U_τ. Keirsbulck et al. (2002) confirmed this result and demonstrated that the normalized stresses collapse outside the roughness sublayer. They also noted that in the inner layer, stresses depend strongly on the roughness. Ligrani and Moffat (1986) noted that the streamwise normal stress was invariant in the outer region when scaled on the friction velocity, while the inner region was invariant only for fully rough flows. Krogstad et al. (1992) noticed a departure of the rough-wall profiles from the smooth-wall profiles over a significant portion of the boundary layer. Bergstrom et al. (2002) also noted a deviation in the mean velocity profiles outside the inner region of the boundary layer. Tachie et al. (2000) noted that the mean velocity profile changed and that the outer peaks in the turbulence profiles flattened out for the rough case.

Few studies have focused on the effects of roughness on a separating flow. For a laminar boundary layer it is well known that roughness delays the separation point by triggering transition. Recent work by Durbin et al. (2001) and Song and Eaton (2002a) showed that separation was very sensitive to upstream roughness, probably due to the increased velocity deficit making the boundary layer less resistant to separation.

The present work attempts to cast light on some of the open questions about roughness effects by independently varying the roughness Reynolds number and the ratio of the roughness height to the boundary layer thickness, k/δ_{99}. The work extends the work of Song and Eaton (2002a) who examined a rough-wall boundary layer that developed on a flat plate then separated as it flowed down a contoured ramp. Both smooth- and rough-wall data have been acquired at two different momentum thickness Reynolds numbers by varying the ambient pressure in the wind tunnel. The roughness size was chosen to maintain the roughness Reynolds number at a constant value, while allowing k/δ_{99} to vary by a factor of four.

2. Experiments

The experiments were performed in a closed loop wind tunnel, which is mounted inside a pressure vessel. The measurements were made with a two component, high-resolution laser Doppler anemometer (LDA) described by DeGraaff and Eaton (2001). The wind tunnel test section has a rectangular cross section and is 152 mm by 711 mm by 2.9 m in length. The flow geometry is shown in Fig. 1. The boundary layer is tripped 150 mm downstream of a 5:1 contraction and develops over a 1.6 m long flat plate. The flow is then mildly contracted over 169 mm on the bottom wall, which reduces the test section height from 152 to 131 mm. The boundary layer then relaxes to equilibrium characteristics on a 320 mm long flat plate. At a typical freestream velocity of 15 m/s, the freestream turbulence level is approximately 0.2%.

The current flow geometry consists of part of the 320 mm flat plate and a smoothly contoured ramp. The ramp has a circular arc with a radius of 127 mm. The ramp expands the tunnel height from 131 to 152 mm. Under smooth-wall conditions there is a separation bubble approximately centered on the ramp's trailing edge, which is 43 mm long. This geometry avoids fixing the separation point on a sharp corner so that, as in many real flows, the separation point occurs on a continuous surface, rather than at a sharp corner.

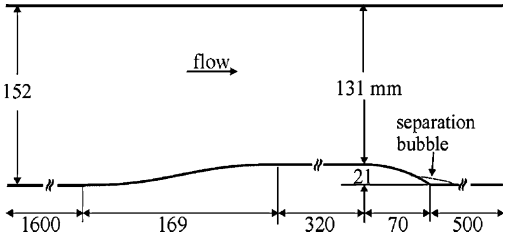

Fig. 1. Flow geometry (not to scale).

The custom LDA has a measurement volume 35 μm in diameter and 60 μm in length. Due to its small measurement volume, two of the major uncertainty sources—velocity gradient bias and two component coincidence are eliminated. The details, including the LDA bias correction, are found in DeGraaff and Eaton (2001). Uncertainties for U, $u'u'$, $v'v'$, $u'v'$ are conservatively estimated, using 5000 samples, as 1.5, 4, 8 and 10% of their local value respectively in the center of the profiles. Near-wall and freestream uncertainties are higher due to the local values approaching zero. Uncertainties are estimated taking into account the statistical uncertainty (5000 samples) and uncertainties in LDA fringe spacing, data filtering, and velocity bias correction. The average data rate varies from about 25 Hz in the freestream for the one atmosphere data sets to about 10 Hz in the freestream for the four atmosphere data sets. For the flat plate location, data sets were taken a minimum of three times and the repeatability of the data sets was better than the uncertainties listed above.

For the rough-wall measurements, two different sandpaper grits were used to establish the two conditions. For the original experiments, 36 grit sandpaper (Norton P36D) was used; for the new work, 120 grit sandpaper (Norton P120CF) was used. The sandpaper was applied from 1.3 m upstream of the ramp to the ramp trailing edge. Control experiments were performed using smooth paper to show that the elevation of the wall position due to the sandpaper thickness has no influence on the flow.

A characteristic height chosen as the average of the local crest heights; k_{ave} was measured for each case. This average local crest height was determined at a number of locations on a sheet of sandpaper using an optical microscope. The measurements were made by bringing into focus the top peak of a sandgrain, recording its relative height based on the microscope's focus setting, and then bringing into focus the paper surface and recording its relative height in the same manner. The difference in these relative heights was considered to be the characteristic height of that grain. These results were then compared with the sandgrain sizes used in the production of the sandpaper, as reported by the manufacturer, and found to match within the uncertainty of the measurements. For the 36 grit sandpaper, the value of k_{ave} was 0.52 mm with a standard deviation of 0.05 mm. This value for the average local crest height is much different than the one reported in Song and Eaton (2002a), due to a difference in measurement technique. The previous technique used a caliper, which preferentially measured the highest peaks on the sandpaper. The optical technique allowed for a more distributed measurement of peak height and avoided preferentially measuring the largest grains. For the 120 grit sandpaper, the value of k_{ave} was 0.13 mm with a standard deviation of 0.01 mm.

3. Results

The results are presented in a Cartesian coordinate system with x being parallel to the upstream flow and y maintained normal to x, even over the curved ramp surface. The normalized coordinate x' denotes a streamwise location normalized with the ramp length, with the origin at the beginning of the ramp. In some plots, the y coordinate is normalized by the ramp height, $h = 21$ mm. Measurements were acquired for four different cases as indicated in Table 1. The two smooth-wall cases were run at one and four atmospheres ambient pressure with freestream velocities near 20 m/s. The increase in pressure from one to four atmospheres produced just under a four-fold increase in the momentum thickness Reynolds number. The two rough-wall cases also were run at one and four atmospheres ambient pressure, again producing approximately a four-fold increase in Re_θ. The roughness heights were chosen to match the roughness height Reynolds number between the two cases. The freestream velocity was lowered to 19.2 m/s for the four-atmosphere case to precisely match the roughness Reynolds number. For the smooth-wall cases a fit of the log law region data was used to determine the value of U_τ. For both rough-wall cases, a method similar to that of Krogstad et al. (1992) and Bandyopadhyay (1987) was used, where both the velocity defect from the wake region and the log law region data were used to estimate the value of U_τ. The uncertainty associated with this method is rather large and must be kept in mind when examining the following scaled data. The uncertainty in U_τ is estimated as 5–10%.

Table 1
Cases examined and roughness parameters

Case	Symbol	U_∞ (m/s)	$P_{ambient}$ (atm)	k_{ave} (mm)	Re_k	Re_{k_s}	$Re_{\theta,ref}$	δ_{99} (mm)	θ (mm)	k_s (mm)	$(\Delta U/U_\tau)$	U_τ (m/s)	τ_{wall} (Pa)
1	□	20.2	1	–	–	–	3400	27.2	2.61	–	–	0.82	0.81
2	■	20.3	4	–	–	–	13200	26.5	2.21	–	–	0.74	3.00
3	○	20.1	1	0.52	42	210	3900	25.2	3.03	2.4	9.65	1.36	2.20
4	●	19.2	4	0.13	39	210	16600	27.7	2.84	0.7	9.58	1.02	5.81

However, it is important to note that all methods used to estimate the value of U_τ in boundary layer flows are subject to similarly large uncertainty.

Flat plate data were measured at $x' = -2.00$, well upstream of any pressure gradient induced by the ramp. Mean velocity profiles at this location are shown in Fig. 2 for all four cases. Overall parameters describing these profiles are shown in Table 1. All four boundary layers have roughly the same overall thickness with δ_{99} values ranging from 25.2 to 27.7 mm. The roughness produces the expected downward shift in the law of the wall plot. The roughness function ($\Delta U/U_\tau$) is approximately equal for the two cases. The equivalent sand grain roughness is $k_s = 2.4$ mm for the one-atmosphere case and $k_s = 0.7$ mm for the four-atmosphere case. These values are approximately five times greater than the actual measured roughness heights. The roughness Reynolds number evaluated using the equivalent sand grain roughness $U_\tau k_s/\nu$ was 210 for both cases, placing them well within the fully rough regime.

The flat plate velocity profiles are plotted as normalized velocity deficit vs y/δ_{99} in Fig. 3. All four profiles are in fairly close agreement for $y/\delta_{99} > 0.05$, especially considering the uncertainty in the friction velocity for the rough-wall cases. A similar collapse of the profiles was observed using the scaling for vertical height proposed by Clauser (1956), $yU_\tau/\delta_{99}U_e$. The Reynolds stress profiles for the flat plate are shown in Fig. 4, where the mixed scaling proposed by DeGraaff and Eaton (2000) for smooth-wall flows has been used.

This scaling has been shown to collapse smooth wall data and results over a wide range of Reynolds numbers, unlike the friction velocity scaling. (Metzger et al., 2001) The wall normal coordinate is normalized by the boundary layer thickness to examine the outer layer

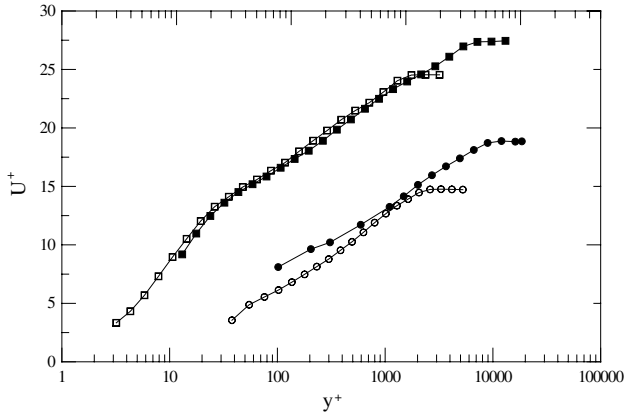

Fig. 2. Law of the wall.

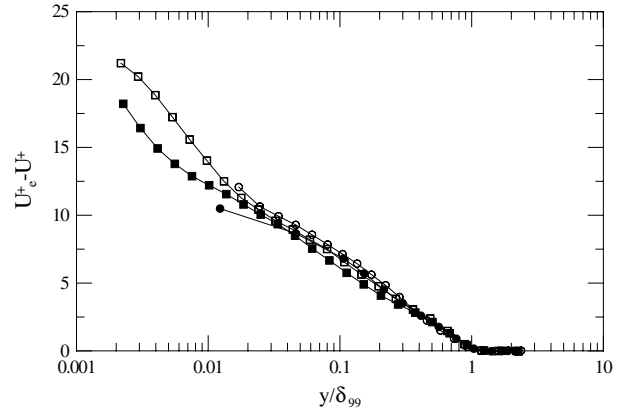

Fig. 3. Mean deficit profile.

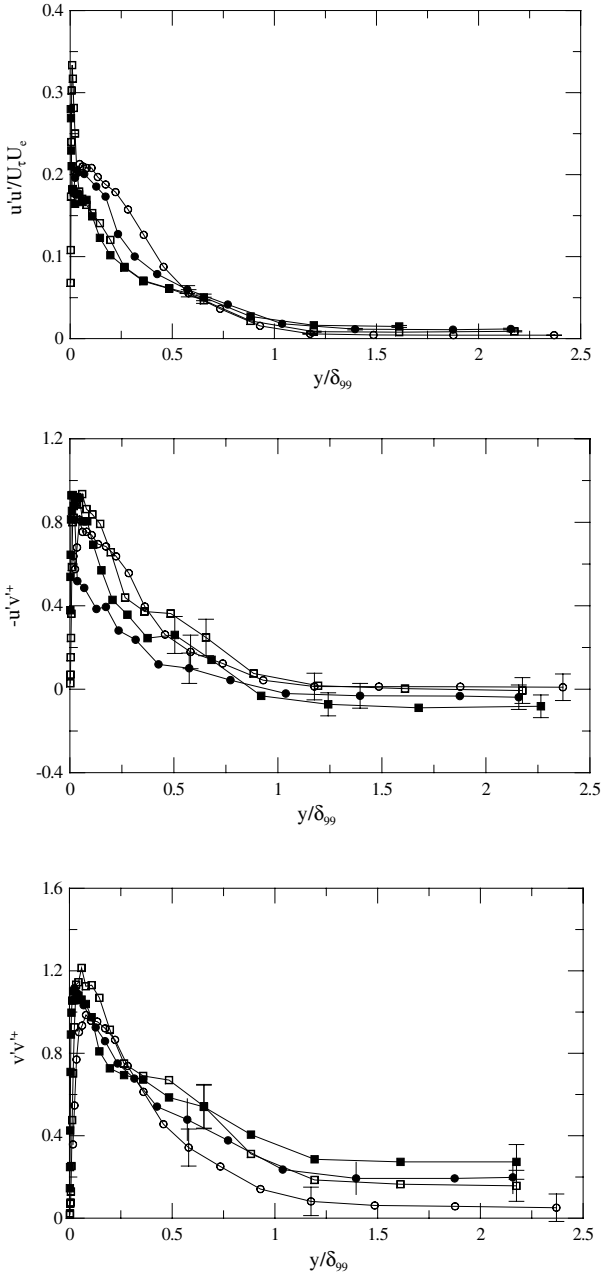

Fig. 4. Reynolds stresses in the upstream boundary layer.

behavior. Generally, the $u'u'$ and $u'v'$ stresses collapse fairly well for $y/\delta_{99} > 0.5$. While there are variations, there is no consistent difference between the smooth and rough-wall cases for the $u'u'$ and $u'v'$ stresses. There is a discernable difference in the $v'v'$ stress measurements where the rough-wall values consistently fall below the smooth wall values. Overall, the mean velocity and turbulence measurements show that the boundary layer structure outside of $y/\delta_{99} = 0.5$ is at most weakly affected by the roughness in so far as the roughness changes the friction velocity. This conclusion is opposite of that reached by Krogstad and Antonia (1999). This disagreement may be due to differences in the roughness types studied.

Two types of measurements were made in the downstream flow to assess the importance of the roughness on flow separation. First, the separation and reattachment points were located; then profiles of the mean velocity and Reynolds stresses were measured for each case at the separation and reattachment points, and at $x' = 0.00$ and 1.00. For the smooth-wall case, the separation point was found by scanning in the streamwise direction at a height of 60 μm above the ramp. Measurements were made every millimeter in the streamwise direction until the separation point was located. The separation point was taken to be the point of zero mean velocity. The same technique was employed for the rough-wall case at four atmospheres although the scanning height was increased to 100 μm. However, for the rough-wall case at one atmosphere the scanning height had to be increased to 800 μm to avoid excessive scatter from glue and sandgrains in the sandpaper. This height was deemed too high, so no separation location is reported for this case. The reattachment points were found in a similar way. For all cases downstream of the ramp the wall was smooth and flat, so the location of the reattachment point is known with the same accuracy for all cases.

The separation and reattachment location measurements are summarized in Table 2. The two smooth-wall cases were essentially identical, indicating that there is no significant effect of Reynolds number on the separation bubble. The separation point for the one-atmosphere rough-wall case is unknown, but other velocity profiles indicated that separation occurred farther upstream than in the smooth-wall case as shown by Song and Eaton (2002a). The reattachment point moved downstream to $x' = 1.76$ for the one-atmosphere rough-wall case versus $x' = 1.36$ for the smooth-wall case. Thus, the separation bubble length increased by at least 65% for this case. The separation point was easier to measure for the high Reynolds number rough-wall case. It was observed to move upstream to $x' = 0.62$. The reattachment point moved to $x' = 1.60$. In other words, the separation bubble for the high Reynolds number, rough case is significantly larger than for the smooth-wall cases, but significantly shorter than for the low Reynolds number rough-wall case.

Table 2
Separation and reattachment points

Case	Separation point	Reattachment point
1	0.74	1.36
2	0.74	1.39
3	–	1.76
4	0.62	1.60

The measured mean velocity profiles for all four cases are shown in Fig. 5. The measurements are normalized by the freestream velocity at $x' = -2.00$. The larger separation bubbles for the rough-wall cases are apparent. Also interesting to note are the differences in the upstream mean velocity profiles using this scaling. While the overall boundary layer thickness is nearly the same for all four cases, it is clear that the velocity deficit is much greater in the middle of the boundary layer for the rough cases. This is especially true for the one-atmosphere rough-wall case, which produces the largest separation bubble.

The development of the wall normal Reynolds stress is seen in Fig. 6. This stress is typical of all three measured stress components. The stress is scaled on the friction velocity at the reference location. The stresses are much larger for the four-atmosphere cases than for the one-atmosphere cases. Overall, the roughness has a similar impact on the Reynolds stresses for both conditions. The adverse pressure gradient of the ramp has less impact on the rough-wall boundary layer, due to the enhanced mixing. The smooth boundary layers develop strong peaks in the Reynolds stresses at the start of the adverse pressure gradient, which then move outward along the ramp. The rough-wall cases develop peaks in the stresses as well, but these peaks are weaker in magnitude and are located farther away from the wall, especially in the region over the ramp.

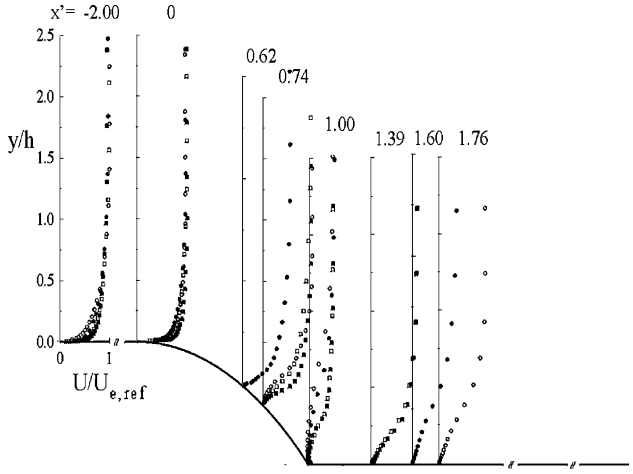

Fig. 5. Mean velocity development.

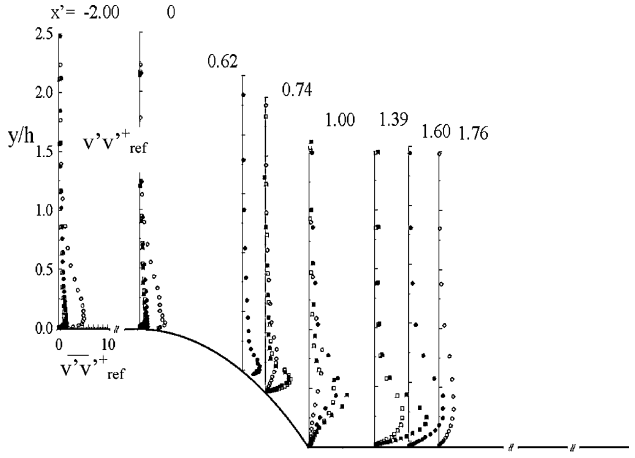

Fig. 6. Reynolds stress development.

The Reynolds stresses at the reattachment point are shown in Fig. 7. The stresses are normalized by the local freestream velocity and the vertical height is normalized by the height of the inflection point in the mean profile. The peak stress levels and the peak heights appear to collapse well between the cases for the same momentum thickness Reynolds number. Those run at the higher Reynolds number are higher than those run at the lower Reynolds number independent of roughness. Similar results are observed at the separation point. Song and Eaton (2002a) showed that the peaks in stresses collapse between the rough and smooth cases at each momentum thickness Reynolds number in this scaling. Since the roughness Reynolds number approaches zero, this shows that the separated shear layer is not affected by the wall conditions.

4. Conclusions

The effects of wall roughness were examined experimentally for two different rough-wall cases over a boundary layer, which developed over a flat plate and then separated and reattached along a ramp. The roughness Reynolds number was matched at two different momentum thickness Reynolds numbers to examine the effect of k/δ_{99} on the flow.

When scaled by the friction velocity, the measured Reynolds stress components are seen to be unaffected by the wall roughness within their uncertainty; this is similar to previous observations by Song and Eaton (2002a). This result contrasts with the work of Krogstad and Antonia (1999) and the difference is probably due to the different characteristics of the roughness elements.

In the separated region, the rough and smooth-wall cases behaved quite differently. For the smooth-wall cases, it has been seen that the separation bubble remains the same size for different momentum thickness

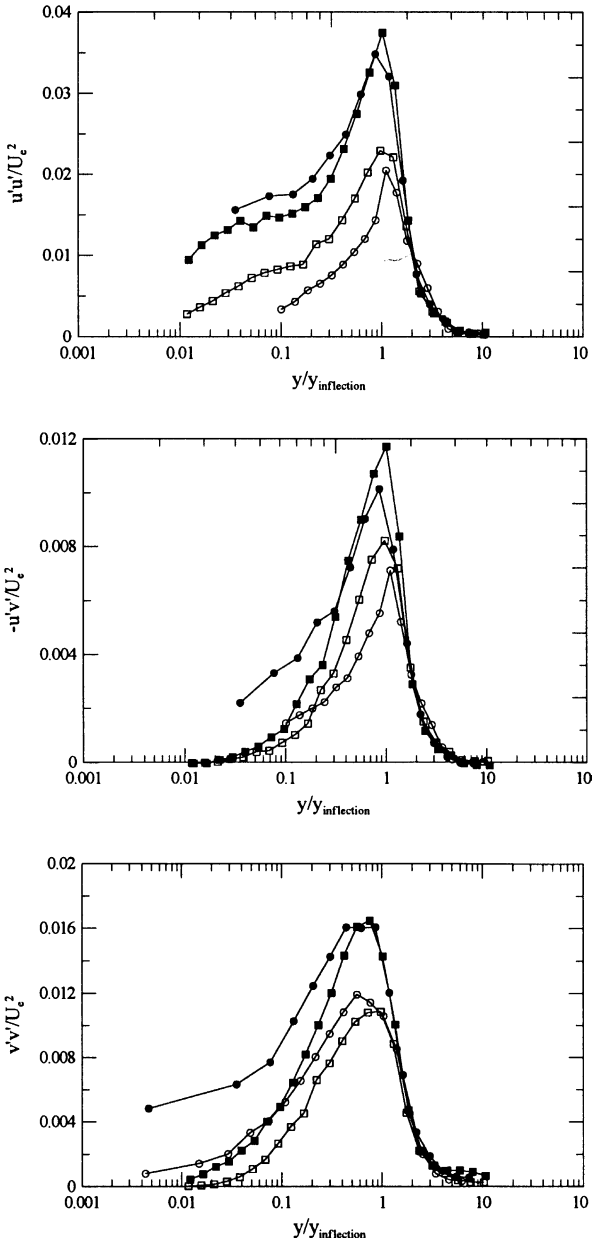

Fig. 7. Reynolds stresses at reattachment.

Reynolds numbers (Song and Eaton, 2002b). The roughness produced a larger separation bubble for both momentum thickness Reynolds numbers but the increase in the size of the bubble was not the same for the two cases. This suggests that another parameter involving the ratio of the boundary layer thickness to the roughness height may be important in the determination of the size of the separation bubble. The roughness acts to increase the momentum deficit in the flat plate, which also affects the separation location and the separation bubble size. The Reynolds stresses normalized by the flat plate friction velocity squared are less sensitive to the adverse pressure gradient for the rough-wall than for the smooth-wall.

Acknowledgements

We gratefully acknowledge the financial support from The Office of Naval Research contract #N00014-00-1-0078. Carolyn Aubertine was partially supported by a National Science Foundation Fellowship.

References

Bandyopadhyay, P., 1987. Rough-wall turbulent boundary layers in the transition regime. Journal of Fluid Mechanics 180, 231–266.

Bergstrom, D., Kotey, N., Tachie, M., 2002. The effects of surface roughness on the mean velocity profile in a turbulent boundary layer. Journal of Fluids Engineering 124, 664–670.

Clauser, F., 1956. The turbulent boundary layer. Advances in Applied Mechanics 4, 1–51.

DeGraaff, D., Eaton, J., 2001. A high resolution laser Doppler anemometer: design, qualification, and uncertainty. Experiments in Fluids 20, 522–530.

DeGraaff, D., Eaton, J., 2000. Reynolds number scaling of the flat plate turbulent boundary layer. Journal of Fluid Mechanics 422, 319–346.

Durbin, P., Medic, G., Seo, J.-M., Eaton, J., Song, S., 2001. Rough wall modification of two-layer k–ϵ. Journal of Fluids Engineering 123, 16–21.

Keirsbulck, L., Labraga, L., Mazouz, A., Tournier, C., 2002. Surface roughness effects on turbulent boundary layer structures. Journal of Fluids Engineering 124, 127–135.

Krogstad, P., Antonia, R., 1999. Surface roughness effects in turbulent boundary layers. Experiments in Fluids 27, 450–460.

Krogstad, P., Antonia, R., Browne, L., 1992. Comparison between rough- and smooth-wall turbulent boundary layers. Journal of Fluid Mechanics 245, 599–617.

Ligrani, P., Moffat, R., 1986. Structure of transitionally rough and fully rough turbulent boundary layers. Journal of Fluid Mechanics 162, 69–98.

Metzger, M.M., Klewicki, J.C., Bradshaw, K.L., Sadr, R., 2001. Scaling the near-wall axial turbulent stress in the zero pressure gradient boundary layer. Physics of Fluids 13, 1819–1821.

Perry, A., Lim, K., Henbest, S., 1987. An experimental study of the turbulence structure in smooth- and rough-wall boundary layers. Journal of Fluid Mechanics 177, 437–466.

Perry, A., Schofield, W., Joubert, P., 1969. Rough wall turbulent boundary layers. Journal of Fluid Mechanics 37, 383–413.

Raupauch, M., Antonia, R., Rajagopalan, S., 1991. Rough-wall turbulent boundary layers. Applied Mechanics Review 44, 1–25.

Smalley, R., Leonardi, S., Antonia, R., Djenidi, L., Orlandi, P., 2002. Reynolds stress anisotropy of turbulent rough wall layers. Experiments in Fluids 33, 31–37.

Song, S., Eaton, J., 2002a. The effects of wall roughness on the separated flow over a smoothly contoured ramp. Experiments in Fluids 33, 38–46.

Song, S., Eaton, J., 2002b. Reynolds number effects on turbulent boundary layer with separation, reattachment, and recovery. TSD Report 146, Stanford University, Stanford, CA.

Tachie, M., Bergstrom, D., Balachandar, R., 2000. Rough wall turbulent boundary layers in shallow open channel flow. Journal of Fluids Engineering 122, 533–541.

Townsend, A.A., 1976. The Structure of Turbulent Shear Flow. Cambridge University Press. 139.